doi:10.22364/mmp2017.18

VIII International Scientific Colloquium
Modelling for Materials Processing
Riga, September 21 - 22, 2017

Mathematical Modeling of Holding Melting Zone with LF and HF EM Fields in Floating Zone Crystal Growth Facilities

A. Krauze, V. Silamiķelis

Abstract

A floating zone facility with EM field pressure supported melting zone is proposed for germanium crystal purification. A test facility is planned to be built at the Institute of Atomic Physics and Spectroscopy at University of Latvia. A simplified analysis of generated EM power and heat transfer shows that aluminum is the best material for the test facility. A 2D axisymmetric, quasi-steady state model for the EM field distribution and free surface shape has also been developed, and first simulation results are presented, including some of the working parameters of the proposed test facility.

Introduction

Along silicon, germanium is an important industrial semiconducting material. One factor that limits its use is its high price. In this article, we consider a floating zone crystal growth facility that could possibly make purification of germanium cheaper.

The facility uses a high-frequency (HF) electromagnetic (EM) inductor to melt a cylindrical column of semiconducting material, see Fig. 1. The molten zone is moved along the column by moving the inductor. Repeated melting of the material will lead to its purification due to impurity segregation process.

Due to large planned column diameter (~100-200 mm), the surface tension will not be able to contain the melt. Although, the HF inductor can create significant pressure on the free surface, it will be localized, in general, at the middle of the melt height. To prevent the melt from spilling out, a maximum pressure at the bottom and zero pressure at the molten zone top should be applied. Such a pressure distribution can be created by a low-frequency (LF) EM inductor. The key problem here is to find an LF inductor configuration that does not produce too large EM power.

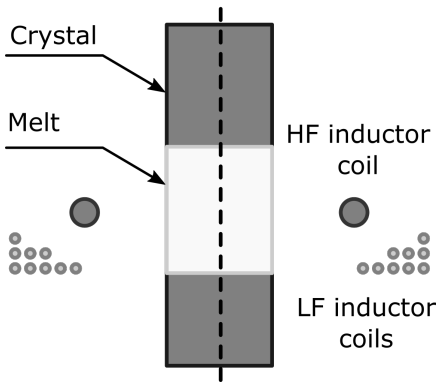

Fig. 1. General scheme for the proposed floating zone crystal growth facility

Institute of Atomic Physics and Spectroscopy at University of Latvia plans to develop a test facility to show feasibility of the method. For this reason, a very simplified heat transfer and EM power generation model was used to determine the best material for the test facility and feasibility of the method for germanium. After that a more sophisticated model that includes simulation of LF and HF EM fields and EM pressure distributions and calculation of free surface shape was developed. The model allowed to calculate the main working parameters of the system, such as inductor current strengths and frequencies. Below we present the description of the models and the main simulation results.

2. Simplified model to determine the right test material

Three materials were considered: tin (Sn), aluminum (Al), and copper (Cu). To compare them, the LF inductor working parameters which ensure the melt containment were determined, and the generated EM power was compared to estimated heat losses from the working material.

A simplified 2D axisymmetric model of the facility with a cylindrical crystal with a molten zone in the middle was considered, see Fig. 2. Crystal diameters from 30 mm to 120 mm were examined. A toroidal LF inductor with triangular cross section was modeled with stranded coil approximation. The frequency was chosen so that the skin-layer depth did not exceed 40% of the crystal radius.

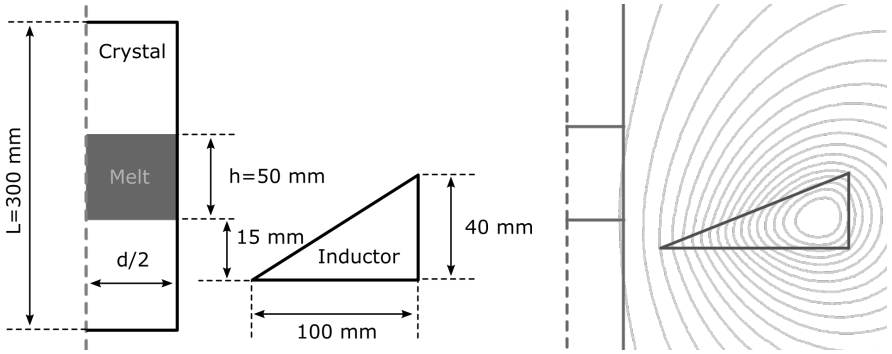

Fig. 2. A simplified model of the test facility. Left: applied dimensions; right: example of a calculated distribution of $A_\varphi r$ for a 60 mm Sn crystal. Simulations carried out with a free finite element program FEMM

The pressure on the free surface was estimated from the distribution of the tangential magnetic field component on the free melt surface, $p_{EM} = |B_\tau|^2/(4\mu_0)$. The inductor current strength was set such that the pressure difference between the bottom and top points were equal to $\rho g h$.

The heat losses due to diffusion in the crystal was estimated as $Q_{ends} = 2S_{cross}\lambda_{sol}(T_0 - T_a)/((L-h)/2)$, where S_{cross} and λ_{sol} are the crystal cross section area and heat conductivity, T_0 is the melting point, and T_a is temperature at the crystal ends. The radiation losses were estimated as $Q_{rad} = S_{side}\sigma_{SB}\varepsilon(T_v^4 - T_a^4)$, where S_{side} is side surface area, σ_{SB} is the Stefan-Boltzmann constant, and ε is surface emissivity, and $T_v = T_0$ is for the melt, and $T_v = (T_0 + T_a)/2$ is for the crystal. In general, radiation losses were small due high metal conductivity. Tab. 1 shows that the best material for the test facility is Al due to its low density.

A series of similar simulations for Ge were also carried out, but with some modifications. The heat losses were modeled via 1D heat transfer model to take into account λ_{sol} temperature dependence, see Tab. 2. The melt zone height was assumed to be equal to the crystal radius. Initial simulations have shown that the LF inductor produced too much power, so two additional coils with opposite wiring direction were introduced. These two coils helped to reduce the magnetic field in the crystal and the generated EM power. Another improvement was a ferromagnetic shield around the HF inductor, which also allowed to reduce the generated LF EM power.

Despite these improvements, the generated LF EM power remains high (~50-58% of the heat losses). This might create significant problems in controlling the melting process, so further optimization of the LF inductor is needed.s

Tab. 1. Applied material properties in simplified LF inductor simulations and obtained simulation results. In Sn 120 mm simulation, the inductor height was increased by 5 mm

Parameter	Sn, 60 mm	Sn, 120 mm	Al, 30 mm	Cu, 30 mm	Ge, 200 mm
σ_{liq}, MS/m	2.78	2.78	4.13	4.76	1.587
σ_{sol}, MS/m	4.48	4.48	9.28	9.83	0.083
λ_{sol}, W/(m · K)	66.8	66.8	211.13	329.4	$\lambda(T)$
ε_{liq} / ε_{sol}	0.5/0.05	0.5/0.05	0.15/0.06	0.15/0.05	0.2/0.55
ρ_{liq}, kg/m^3	6990	6990	2375	7955	5570
T_0, K	505.08	505.08	933.47	1257.77	1211.4
Frequency, Hz	150	150	1500	1500	100
Heat losses, W	721	2845	1618	4212	9267
EM power, W	709	2390	414	1399	5482
Ratio	0.98	0.84	0.26	0.33	0.58

Tab. 2. Heat conductivity for germanium as it was used in the simulations

T, K	250	300	350	400	500	600	800	1000	1200
λ_{sol}, W/(m · K)	74.9	59.9	49.5	43.2	33.8	27.3	19.8	17.4	17.4

3. Modeling free surface shape and facility working parameters

3.1. Low-frequency EM field model

To better determine the working parameters of the test system, a 2D axisymmetric, quasi-steady state model was developed, in which the free surface shape changes were also modeled. 30 mm Al crystal was considered. The geometry of the LF inductor is now modeled more precisely. 6 mm diameter tubes, placed 8 mm from each other, were used for the main inductor coil as well as for the two coils with the opposite wiring, see Fig. 3.

The ferromagnetic shield was also modeled. The main reason for its use is to reduce the HF inductor influence on the LF inductor. Its side thickness was set to 10 mm to reduce the magnetic field concentration in it below 0.4 T. The shield is used both in the HF and LF simulations with the same $\mu = 18$ value.

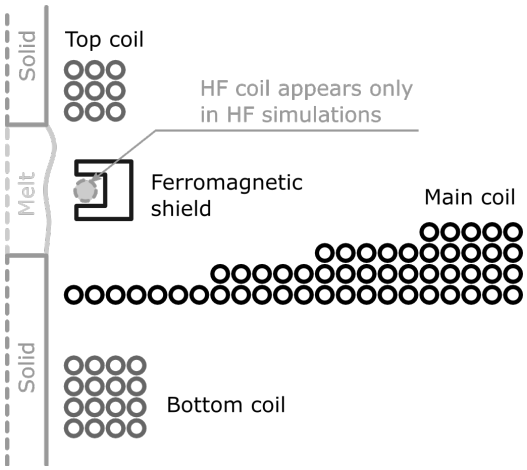

Fig. 3. Geometry of the modeled system in LF EM simulations. The HF inductor is modeled in a separate HF EM field simulation

An equation for the azimuthal component of the magnetic vector potential is solved:

$$\nabla \times \left(\frac{1}{\mu\mu_0} \nabla \times A_\varphi \vec{e}_\varphi \right) = -i\sigma\omega A_\varphi \vec{e}_\varphi + \vec{j}_s, \qquad (3.1)$$

where $\vec{j}_s$ represents the current density in the inductor coils (the stranded coil model). 1500 Hz frequency is used in the simulations.

The pressure distribution in the melt is calculated from the potential part of the EM force acting on the melt, and the EM power density distribution is calculated from the current density distribution:

$$p_{EM,LF} = -\frac{|\vec{B}|^2}{4\mu_0}, \qquad q_{EM,LF} = \frac{|\vec{j}|^2}{2\sigma}. \tag{3.2}$$

3.2. High-frequency EM field model

750 kHz frequency is used for the HF inductor. At this frequency, the skin-layer depth in Al and Cu is much smaller than the geometric dimensions of the growth facility parts, so the equation for A_φ is solved only for the air:

$$\nabla \times \left(\frac{1}{\mu\mu_0} \nabla \times A_\varphi \vec{e}_\varphi \right) = 0, \tag{3.3}$$

Zero boundary condition was applied on the Al surface, $A_\varphi r = 1$ was applied on the HF inductor coil. Individual boundary conditions $A_\varphi r = a_i$ are applied to the LF inductor tube boundaries. Values a_i are chosen so that the total HF current strength I_i in a wire i were equal to zero.

The EM pressure distribution on the free surface and the EM power density distribution on all surface is calculated according to formulas of the 1D skin-layer model:

$$p_{EM,LF} = \frac{\mu_0 |\vec{i}|^2}{4}, \qquad q_{EM,LF} = \frac{|\vec{i}|^2}{2\sigma\delta}, \tag{3.4}$$

where $\vec{i}$ denotes surface current density, and δ is the skin-layer depth. After that the pressure and power density distributions are scaled to make a total generated EM power equal to 1300 W. Since the LF inductor induces additional ~200-300 W, the total induced power is approximately equal to the heat losses from the working material.

3.3. Free surface model

A stationary free surface shape is calculated by requiring that sum of all forces acting on any of its points is zero:

$$p_\gamma + p_{EM} + \rho_{liq} g (z_{\max} - z) + p_0 = 0, \tag{3.5}$$

where p_γ is surface tension pressure, p_{EM} is the total EM pressure, z is the vertical coordinate, and p_0 is a constant term that characterizes general melt compression. The free surface shape is obtained iteratively. First, pressure discrepancies Δp_i are calculated for each free surface node:

$$\Delta p_i = p_{\gamma,i} + p_{EM,i} + \rho_{liq} g (z_{\max} - z) + p_0, \tag{3.6}$$

Surface nodes are shifted in the radial direction, $\Delta r_i = c \Delta p_i$, where c is some constant. Also, the surface tension term is linearized against the node shifts:

$$p_{\gamma,i} \approx p^0_{\gamma,i} + \frac{\partial p_{\gamma,i}}{\partial r_j} \Delta r_j. \tag{3.7}$$

When these two expressions are inserted into the pressure discrepancy expression, a system of linear algebraic equations for the shifts is obtained: $\Delta r_i = A_{ij}\Delta r_j + B_i + cp_0$. The solution for this system is linear expressions for the shifts in the form: $\Delta r_i = A_i' p_0 + B_i'$.

The unknown p_0 is obtained by requiring that the melt volume is kept constant. Assuming homogeneous vertical spacing between the surface nodes and horizontal crystallization interfaces, the melt volume can be calculated as $V = \pi/3\Delta z \sum \left(r_i^2 + r_i r_{i+1} + r_{i+1}^2\right)$, where summation occurs over all segments. Inserting the expression for the node shifts into produces a quadratic equation $V = Ap_0^2 + Bp_0 + C$. One root of this equation gives a physical meaningful surface shape.

3.4. Numerical implementation of the model and simulation results

The EM field models are solved with a free finite element program *getdp* [1]. Triangular meshes for EM field simulations were generated with a free mesh generation program *gmsh,* [2]. The iterative procedure for obtaining the free surface was implemented in a *python* language script. Fig. 4 shows a block scheme of the implemented algorithm.

Fig. 4 also shows the calculated free surface shapes for different LF inductor current strengths and an example of calculated LF EM field and pressure distribution. Fig. 5 shows some of the calculated dependencies of the system parameters. For example, one can see that the LF inductor current should be change by up to 20% in order to change the meniscus angle at triple points and control the crystal growth. The induced LF EM power increases by 60 W in the process, which constitutes only 4% of the total power. The HF inductor parameters remain almost unaffected; the HF inductor current changes just by 3%.

A transient version of the model is being developed. It will include heat transfer simulations to model correctly crystal melting and crystallization interface shapes. When development of such model is finished, it will allow to model the stability of the molten zone form and therefore the applicability of the proposed crystal growth method for Ge purification.

Conclusions

Simplified heat transfer and EM power simulations have shown that aluminum is the best suitable material for a test implementation of a floating zone crystal growth facility in

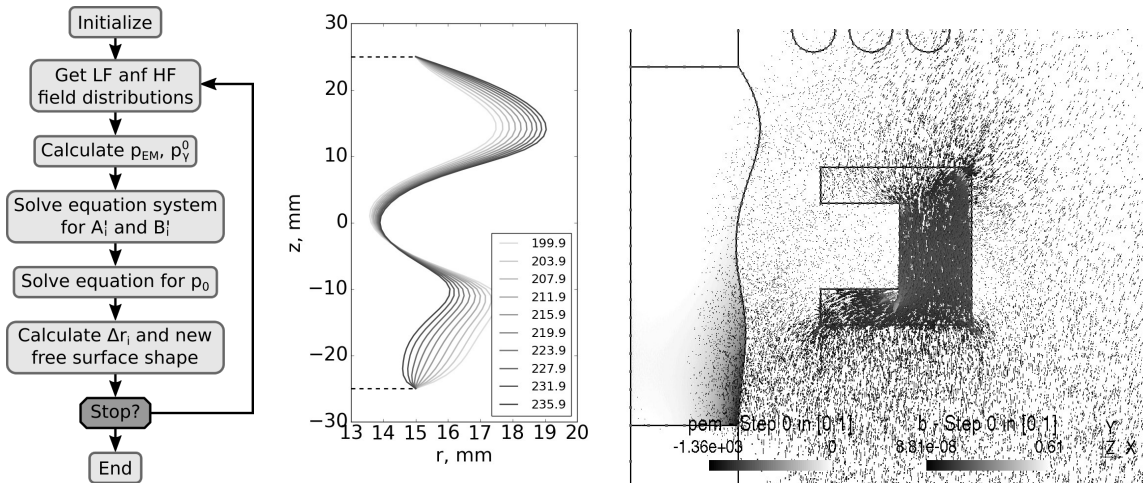

Fig. 4. Left: block scheme of the simulation algorithm. Middle: calculated free surface shapes for different LF inductor current strengths. Right: example of LF simulation results, real part of LF magnetic field and EM pressure in the melt

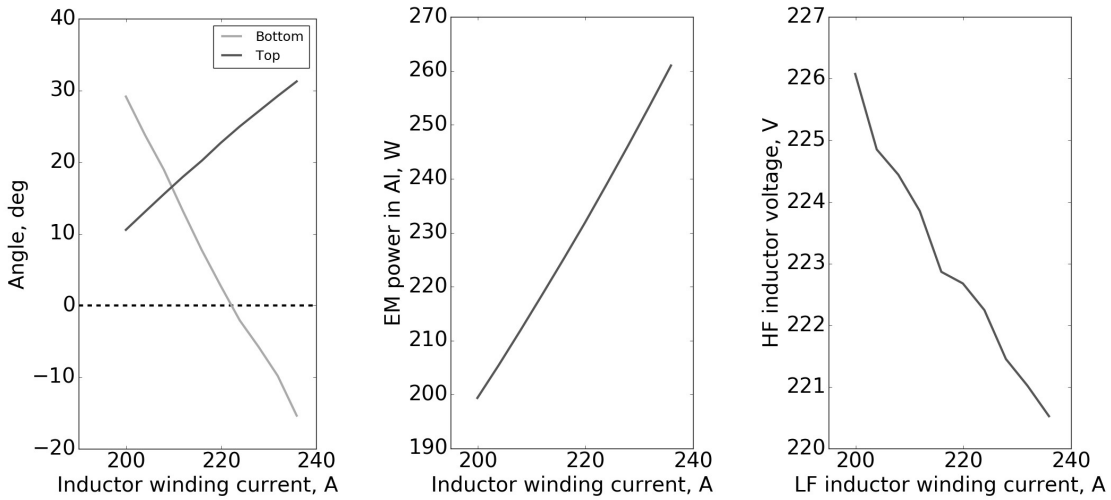

Fig. 5. Example of calculated parameter dependencies on the LF inductor current strength. Left: meniscus angles at the top and bottom triple points. Middle: EM power generated by the LF inductor in Al. Right: HF inductor voltage

which the melt zone is held by EM field pressure. It was shown that the proposed facility could be used for germanium; however, a considerable optimization of the facility must be carried out.

A more complex model for the free surface shape simulation was also developed. The model allows to determine the basic working parameters of the facility, such as LF and HF inductor current strengths.

Acknowledgements

The Effective Cooperation project Nr. AAP2016/B088 of University of Latvia "Research on application MHD levitation in large size high-purity crystal growth" was financed by University of Latvia and BSI Ltd company. We would like to thank the CEO of BSI Ltd, V. Gastillo, for the financial support, Ā. Veispals for invaluable scientific knowledge, as well as A. Ūbelis and other members of the laboratory for helping the project to come to life.

References

[1] Geuzaine, C.: *GetDP: a general finite-element solver for the Rham complex*. Sixth International Congress on Industrial Applied Mathematics (ICIAM07) and GAMM Annual Meeting, PAMM Vol. 7, Issue 1. Special Issue. Zuerich 2007, Wiley, pp. 1010603--1010604.

[2] C. Geuzaine, J.-F. Remacle. *Gmsh: a three-dimensional finite element mesh generator with built-in pre- and post-processing facilities*. International Journal for Numerical Methods in Engineering 79(11), pp. 1309-1331, 2009.

Authors

Dr. Phys. Krauze, Armands
Laboratory for mathematical modelling of environmental and technological processes
University of Latvia
Zeļļu str. 23
LV-1002 Riga, Latvia
E-mail: armands.krauze@lu.lv

MSc. Viesturs Silamiķelis
Institute of Atomic Physics and Spectroscopy
University of Latvia
Raiņa blvd. 19
LV-1586 Riga, Latvia
E-mail: viesturs.silamikelis@gmail.com